Original Research

Curcumin attenuates vascular calcification via the exosomal miR-92b-3p/KLF4 axis

Chuanzhen Chen[1]* iD, Yaodong Li[2]*, Hailin Lu[1]*, Kai Liu[1], Wenhong Jiang[1], Zhanman Zhang[1] and Xiao Qin[1] iD

[1]Department of Vascular Surgery, The First Affiliated Hospital of Guangxi Medical University, Nanning 530021, China; [2]Department of Vascular Surgery, Tianjin Hospital, Tianjin 300211, P.R. China
Corresponding author: Xiao Qin. Email: dr_qinxiao@hotmail.com
*These authors contributed equally to this work.

Impact Statement

Vascular calcification (VC) underlies the pathophysiology of multiple diseases and is a major risk factor for cardiovascular disease. Therefore, understanding the pathogenesis of VC and identifying potential therapeutic targets is urgently required. This study showed that curcumin (CUR) attenuated VC by affecting exosomes secreted by vascular smooth muscle cells (VSMCs). Exosomes can be absorbed by vascular smooth cells and act via the miRNAs they carry. We found that the high expression of miR-92b-3p in exosomes secreted after CUR intervention had a major effect of alleviating VC. The miR-92b-3p/KLF4 axis was involved in the pathological regulation of VC. Moreover, CUR attenuated VC by increasing miR-92b-3p expression and decreasing KLF4 expression *in vivo*. This study provides a new option for the treatment and prevention of VC.

Abstract

Vascular calcification (VC) is the most widespread pathological change in diseases of the vascular system. However, we do not have a good understanding of the molecular mechanisms and effective therapeutic approaches for VC. Curcumin (CUR) is a natural polyphenolic compound that has hypolipidemic, anti-inflammatory, and antioxidant effects on the cardiovascular system. Exosomes are known to have extensive miRNAs for intercellular regulation. This study investigated whether CUR attenuates VC by affecting the secretion of exosomal miRNAs. Calcification models were established *in vivo* and *in vitro* using vitamin D3 and β-glycerophosphate, respectively. Appropriate therapeutic concentrations of CUR were detected on vascular smooth muscle cells (VSMCs) using a cell counting kit 8. Exosomes were extracted by super speed centrifugation from the supernatant of cultured VSMCs and identified by transmission electron microscopy and particle size analysis. Functional and phenotypic experiments were performed *in vitro* to verify the effects of CUR and exosomes secreted by VSMCs treated with CUR on calcified VSMCs. Compared with the calcified control group, both CUR and exosomes secreted by VSMCs after CUR intervention attenuated calcification in VSMCs. Real-Time quantitative PCR (RT-qPCR) experiments showed that miR-92b-3p, which is important for alleviating VC, was expressed highly in both VSMCs and exosomes after CUR intervention. The mimic miR-92b-3p significantly decreased the expression of transcription factor KLF4 and osteogenic factor RUNX2 in VSMCs, while the inhibitor miR-92b-3p had the opposite effect. Based on bioinformatics databases and dual luciferase experiments, the prospective target of miR-92b-3p was determined to be KLF4. Both mRNA and protein of RUNX2 were decreased and increased in VSMCs by inhibiting and overexpressing of KLF4, respectively. In addition, in the rat calcification models, CUR attenuated vitamin D3-induced VC by increasing miR-92b-3p expression and decreasing KLF4 expression in the aorta. In conclusion, our study suggests that CUR attenuates vascular calcification via the exosomal miR-92b-3p/KLF4 axis.

Introduction

Vascular calcification (VC) increases with age, with chronic kidney disease, hypertension, and diabetes all contributing to this process.[1] VC occurs mainly in the intima and middle layers of the aorta and was initially thought to be a passive process, referring mainly to deposition of calcium phosphate minerals on the intima of arteries.[2,3] However, phenotypic switching of vascular smooth muscle cells (VSMCs) in the mid-vascular layer was shown recently to act as an essential factor in regulating VC.[1,4] Vascular smooth muscle cells are transformed to be an osteoblast phenotype after disease, with this alteration decreasing the VSMC makers, SM22α and SMα-actin, and increasing bone formation markers, RUNX2 and alkaline phosphatase (ALP).[5,6]

Curcumin (CUR) is a natural polyphenol extracted from the plant turmeric. Ongoing research on CUR's action has shown it has anti-inflammatory, antioxidant, anti-tumor,

hypolipidemic, and anti-atherosclerotic effects, with minimal toxic side effects.[7–10] It has also been reported that CUR inhibits apoptosis of VSMCs[11] and is involved in regulating VC[12,13] by inhibiting JNK/Bax signaling pathway-mediated apoptosis.[14] While there is increasing evidence that CUR can protect the cardiovascular system,[15,16] the molecular mechanism by which CUR attenuates VC remains unknown.

Exosomes (EXO) have been found in calcified human aortic valves and in the aortic mesentery.[17] Exosomes are extracellular vesicles, sized between 30 to 150 nm, that are secreted by various cell types and contain miRNA, mRNA, and proteins for intercellular communication.[18] Normally, VSMCs secrete exosomes to regulate other cells. However, in disease conditions, calcified VSMCs also secrete exosomes that affect the growth of normal VSMCs, thereby exacerbating VC.[19–23] On the basis of this finding, we undertook a study to verify whether CUR attenuated VC through a mechanism affecting exosome secretion.

Materials and methods

Ethical statements

All the animal experiments were approved by the Ethics Committee of Guangxi Medical University (Approval Number: 201910033). The study conformed to the guidelines for the care and use of laboratory animals published by the Chinese Academy of Health Sciences.

Reagents

Curcumin (A0086) was obtained from Chengdu Must Biotechnology Co., Ltd, China. β-glycerophosphate (50020), PKH26 (PKH26PCL), and GW4869 (D1692) were bought from Sigma-Aldrich (St. Louis, MO, USA), while the NucleoZOL RNA isolation kit (740404) was purchased from Macherey-Nagel (Düren, Germany). DMEM culture medium (319-006-CL) was purchased from Wisent Biotechnology (Canada) and Runx2 (ab23981, 1:1000) from Abcam (Cambridge, MA, USA). GAPDH (60004-1-Ig, 1E6D9, 1:20000), KLF4 (11880-1-AP, 1:500), and ASMA (14395-1-AP, 1:1000) were purchased from Proteintech (Wuhan, China), the mRNA RT-qPCR detection kit (R323-01) from Nanjing Vazyme Biotech Co., Ltd, China, and the miRNA RT-qPCR detection kit (QP115) and all primers used in this study from GeneCopoeia (Guangzhou, China). KLF4 siRNA (siB0858163956-1-5), miR-92b-3p mimic (miR10005340-1-5), the inhibitors miR-92b-3p (miR20005340-1-5), and their corresponding comparators were purchased from Guangzhou RiboBio Co., Ltd, China. Overexpressed (OE) KLF4 plasmid was purchased from Shanghai Genechem Co., Ltd, China. The ALP assay kit (P0321 S), alkaline phosphatase color development kit (C3206), Alizarin Red S staining solution (C0140), calcium colorimetric assay kit (S1063 S), cell counting kit-8 (C0038), DAPI (C1105), Western and IP cell lysate (P0013J) were purchased from Beyotime (Shanghai, China). Fetal bovine serum (10099133C), the Bicinchoninic Acid (BCA) protein assay kit (23225), and Lipofectamine™ 3000 transfection reagent were purchased from Thermo Fisher Scientific (Waltham, MA, USA). The enhanced chemiluminescent (ECL) reagent kit (BL520A) was obtained from

Biosharp (Shanghai, China) and exosome-free fetal bovine serum (C38010050) from Biological Industries (Kibbutz Beit Haemek, Israel).

Cell culture and interventions

Rat VSMCs were bought from Kunming Cell Bank, Chinese Academy of Sciences, and cultured in DMEM medium containing 10% fetal bovine serum and 1% penicillin/streptomycin in a fixed environment at 37°C and 5% CO_2. The medium was updated each 2 days to promote better cell growth. To establish a model of calcification of VSMCs, the cells were induced in DMEM medium containing 10 mM β-glycerophosphate (β-GP). CUR was dissolved in DMSO and co-intervened for 14 days with VSMCs induced by calcification to determine the regulatory effect of CUR on calcification. Transient transfection of KLF4 siRNA with overexpressed KLF4 plasmid, miR-92b-3p mimics, and suppressors was carried out in VSMCs in six plates using Lipo3000TM based on the manufacturer's instructions. All the experiments were conducted separately for a minimum of three times.

Toxicity analysis of CUR

The toxic effect of CUR on VSMCs was determined using the cell counting kit 8. VSMCs were inoculated into 96-well cell culture plates at a density of 1500 cells per well according to the manufacturer's directions. After the addition of different concentrations of CUR (0, 0.1, 1, 10, and 100 μM) to the VSMCs, the absorbance at 450 nm was analyzed at 24 h and 48 h using an enzyme marker.

Isolation, purification, and identification of exosomes

To exclude the interference of exosomes in fetal bovine serum and to collect only exosomes secreted by VSMCs, we cultured VSMCs in DMEM medium prepared with exosome-free fetal bovine serum. After 48 h of incubation, differential centrifugation was used to collect the cell supernatant for isolation and purification of the exosomes. This involved centrifugation at 300 g for 10 min and then 2000 g for 10 min to clear the suspended cells, followed by centrifugation at 10,000 g for 30 min to remove cell debris, and then by ultracentrifugation at 110,000 g for 90 min. The exosomes were treated once with phosphate buffered saline (PBS), centrifuged again at 110,000 g for 90 min, and finally mixed in PBS. According to the manufacturer's directions, we measured the protein levels of exosomes using the BCA protein assay kit. A transmission electron microscope (Hitachi HT7800, Japan) was used for morphological analysis and a nanoparticle tracking analyzer Zetaview (Particle Metrix, Germany) for particle size analysis of the exosomes. The marker protein for exosomes, TSG101, was measured using western blotting. The exosomes were labeled with PKH26 to observe their uptake by VSMCs using a confocal microscope (Leica TCS SP8, Germany) according to the manufacturer's directions.

RT-qPCR experiments

Total RNA was obtained from aortic tissue and VSMCs using the NucleoZOL RNA isolation kit, according to the maker's

directions. To measure the expression of miR-92b-3p, KLF4, and RUNX2, the extracted RNA was subjected to reverse transcription and the real-time fluorescence polymerase chain reaction using ABI 7500 Fast (Applied Biosystems, Darmstadt, Germany).

RUNX2 forward 5′-CATGGCCGGGAATGATGAG-3′ and reverse 5′-TGTGAAGACCGTTATGGTCAAAGTG-3′; KLF4 forward,5′-CGGGAAGGGAGAAGACACTGC-3′ and reverse 5′-GCTAGCTGGGGAAGACGAGGA-3′; β-actin forward 5′-GGAGATTACTGCCCTGGCTCCTA-3′ and reverse 5′-GACTCATCGTACTCCTGCTTGCTG-3′; miR-92b-3p(CGCAGTATTGCACTCGTC). miR-7a-5p(TGGAAGACTAGTGATTTTGTTGTAAA). KLF4 and RUNX2 expressions were normalized by β-actin and miR-92b-3p expression by U6, with the relative expressions calculated by comparison with the 2-ΔΔCT method. All experiments were repeated three times independently.

Western blotting

We extracted proteins from the VSMCs and determined the protein concentrations using the BCA protein assay kit. An equivalent quantity of protein sample (20 μg) was then electrophoresed and transferred to polyvinylidene fluoride (PVDF) membranes. We closed the strips with 5% skim milk powder for 1h, followed by incubation with a primary antibody (RUNX2, KLF4, or GAPDH) at 4°C overnight. The membranes were washed the next day and soaked with the appropriate secondary antibody for 1h at room temperature, followed by detection using the FluorChem FC3 (ProteinSimple, San Jose, CA, USA) imaging system in conjunction with the ECL chemiluminescent substrate kit. The protein expression was then quantified using Image J. All experiments were repeated three times independently.

Cellular Alizarin Red S staining, ALP staining, and activity assay

Six-well plates containing VSMCs were flushed lightly with PBS, followed by the addition of 4% paraformaldehyde for 10 min. Calcium ions were detected by staining with an Alizarin Red S solution for 10 min, according to the manufacturer's directions. After staining with the ALP color development kit for 30 min, photographs were taken under a light microscope and the results were analyzed by Image J.

For measurement of ALP activity, six-well plates of cultured cells were washed lightly three times and lysed by adding 100 μL of Western and IP cell lysis solution. According to the manufacturer's directions, we used the ALP assay kit to measure ALP activity and the BCA assay kit to measure protein density. ALP activity was expressed relatively by protein levels as U/mg of protein.

Immunofluorescence

We used 4% paraformaldehyde to fix the VSMCs for 10 min and 0.1% Triton X-100 to penetrate the cells for 10 min, closed them with 10% bovine serum albumin blocking solution, and then incubated them with primary antibody at 4°C overnight. The next day, the cell surface was rinsed gently with PBS and immersed with the corresponding fluorescent secondary antibody for 1h at room temperature. The cells were

then soaked in the DAPI solution for 10 min. An inverted fluorescence microscope (IX71-olympus, Japan) was used to observe the fluorescence of the cellular proteins.

Transwell co-culture system

To verify the role of the secreted exosomes affecting VSMCs after CUR intervention, we cultured VSMCS using the Transwell co-culture system (Corning-3450, NY, USA). In this system, both the upper and lower chamber of the culture dish are used to grow the VSMCs. We used CUR-containing medium for VSMCs in the lower chamber, with or without GW4869 (an exosome secretion inhibitor). The changes in the VSMCs in the upper chamber of the petri dish were analyzed after 48 hr.

Luciferase reporter assay

The online public databases (miRDB (http://mirdb.org/index.html) and Targetscan (http://www.targetscan.org)) were used to identify possible mRNA binding sites that were regulated by rat miR-92b-3p. After examining the intersection analysis of the results, we considered that KLF4 was a significant binding target. To further determine the regulatory relationship between miR-29b-3p and KLF4, we performed a dual-luciferase reporter gene assay in HEK293T cells. In this experiment, we transfected wild-type KLF4 3′-UTR or mutant KLF4 3′-UTR and miR-92b-3p mimics or the relative controls in HEK293T cells. A luciferase detection system (Promega Corporation, Madison, Wisconsin, USA) was used to analyze firefly luciferase activity, according to the manufacturer's directions.

Animal research

We obtained male Sprague Dawley rats aged about 3 months with an average weight of 200 g from the Experimental Animal Center of Guangxi Medical University for the studies. The animals were divided randomly into three groups each containing five animals. A rat model of VC was established by intraperitoneal injection of vitamin D3 (Vit D3) 300,000 IU/kg once daily for 14 days and represented the calcification control group. Negative control rats were administered equal amounts of saline by the same route for the same duration. In the CUR treatment group, in addition to the dose of Vit D3 received by the calcified control group, 50 mg/kg of CUR dissolved in olive oil was added daily by gavage for 14 days. To comply with the univariate principle of the experiment, the negative control and calcified control groups were administered equal amounts of olive oil by gavage. At the end of the experiment, the rats were executed by cervical dislocation and their thoracic aorta collected. Followed by fixation of the specimen, 8 mm sections were prepared for Alizarin Red S staining, Von Kossa staining, and the immunohistochemical experiments. RNA and protein were extracted from the other aortic structures.

Alizarin Red S staining, Von Kossa staining, and immunohistochemistry of the aorta

The thoracic aorta was fixed in 4% paraformaldehyde for 24 hr, immersed in wax, and then sliced into 8 mm thick sections as described previously.[24] Xylene was used to dewax the

sections, followed by dehydration in an alcohol solution. For Alizarin Red S staining, the sections were placed in the staining solution for 5 min, according to the manufacturer's directions, and then photographed under a light microscope. For the Von Kossa staining, we incubated the sections in 1% silver nitrate in the sunlight for 1 h, then in 5% sodium thiosulfate for 2 min, and then photographed with a light microscope,[25] according to the manufacturer's directions. Positively stained areas were detected using Image J analysis.

For immunohistochemical staining of rat thoracic aorta, the tissue was cut into 5 μm size sections as described previously.[26] Briefly, the sections were stripped of wax, dehydrated in graded alcohol solutions, closed with 5% fetal serum for 1 h and the immersed overnight in primary antibodies for KLF4 and RUNX2 at 4°C. The sections were then incubated with the corresponding secondary antibody at room for 1 h and treated with the Diaminobenzidine (DAB) kit, according to the manufacturer's guidelines. The nuclei were stained with hematoxylin, followed by photography using a light microscope (Nikon ECLIPSE CI, Japan). Image J was used for analysis of the positively stained areas.

Statistical analysis

All the results were presented as mean ± SD. Statistical analysis of the experimental data of two sample groups was performed using Student's unpaired t test and one-way analysis of variance for ≥3 groups using GraphPad Prism (version 8.0, CA, USA). The correlation between KLF4 and miR-92b-3p expression was analyzed using Pearson correlation analysis. Statistical significance was defined as p values < 0.05.

Results

CUR attenuates the calcification of VSMCs

As shown in Figure 1(A), CUR concentrations of 0.1 μM, 1 μM, and 10 μM had no statistically significant effect on the growth of VSMCs, although the concentration of 100 μM CUR had a significant toxic effect on growth. We found that 10 μM CUR was most effective in attenuating the calcification of VSMCs. RT-qPCR showed that 10 μM CUR inhibited the expression of RUNX2 mRNA in a dose-dependent manner (Figure 1(B)). Meanwhile, western blot analysis also showed that expression of RUNX2 protein was dose-dependently inhibited by 10 μM CUR (Figure 1(C)). We therefore used a concentration of 10 μM for all interventions with CUR in later studies. We also showed that osteogenic differentiation and calcification of VSMCs were inhibited after CUR treatment using the ALP activity assay (Figure 1(D)), Alizarin Red S staining (Figure 1(E)), and alkaline phosphatase staining (Figure 1(F)). These studies demonstrated that CUR attenuated calcification in VSMCs.

Secretion of exosomes after CUR intervention in VSMCs attenuates the calcification of VSMCs

Exosomes isolated from the cell supernatant of VSMCs incubated with CUR were analyzed to determine whether they affected the calcification of VSMCs. Transmission electron microscopy showed that these vesicles had a typical cup-shaped or spherical morphology (Figure 2(A)). Nanoparticle

tracking analyzer analysis confirmed that most VSMCs secreted exosomes, sized about 30–150 nm (Figure 2(B)). Western blot analysis showed that TSG101, a protein marker for exosomes, was expressed significantly in these vesicle enrichments compared with that in the cell supernatant (Figure 2(C)). These findings confirm that we had extracted exosomes from the cell supernatant.

To investigate whether the exosomes excreted by VSMCs after CUR intervention were absorbed by other VSMCs, we used PKH26 to label the exosomes. The labeled exosomes were then incubated with VSMCs. We used confocal microscopy to show that the labeled exosomes could be absorbed by VSMCs (Figure 2(D)). To investigate whether exosomes secreted after incubation of VSMCs with CUR inhibited the calcification of VSMCs, we collected cell supernatants of the cultures and isolated the exosomes by differential centrifugation. These exosomes were shown to inhibit the calcification of other VSMCs using RUNX2 mRNA expression (Figure 2(E)), Alizarin Red S staining (Figure 2(F)), ALP staining (Figure 2(G)), and ALP activity assay (Figure 2(H)).

CUR affects exosomes secreted by VSMCs to attenuate the calcification of VSMCs

To confirm whether the exosomes secreted after incubation of VSMCs with CUR inhibited calcification, VSMCs were cultured in an exosome-free fetal bovine serum medium. The following subgroups were prepared for the experiment. The negative control was VSMCs without any intervention, while the experimental groups included VSMCs incubated with CUR with or without GW4869, an exosome secretion inhibitor. As shown in Figure 3(A) to (C), the addition of CUR attenuated osteogenic differentiation (Figure 3(A)) and alkaline phosphatase activity (Figure 3(B)) in VSMCs compared with that observed in negative controls. The marker protein (alpha-smooth muscle actin (ASMA)) was increased in VSMCs (Figure 3(C)), although these inhibitory effects disappeared after the addition of GW4869. These results showed that CUR impairs the calcification of VSMCs due to its effect on the exosome secretion from VSMCs.

To verify the mutual regulation of secretory exosomes in VSMCs, the cells were cultured in the Transwell co-culture system using an exosome-free fetal bovine serum medium. As shown in Figure 3(D), VSMCs in the lower chamber of this system were incubated with CUR, with or without GW4869, while normally growing VSMCs were co-cultured in the upper chamber. The results indicated that RUNX2 mRNA expression (Figure 3(E)) and ALP activity (Figure 3(F)) were increased in VSMCs in the upper chamber and in the lower chamber containing GW4869, compared with cells with no addition of GW4869. These data confirm that exosomes interact among VSMCs and are influenced by GW4869. In summary, CUR affects exosomes secreted by VSMCs, thereby impairing the calcification of VSMCs.

### CUR increases miR-92b-3p expression in exosomes and VSMCs to suppress calcification of VSMCs

Numerous reviews have indicated that exosomes excreted by VSMCs are enriched with miRNAs and that these miRNAs
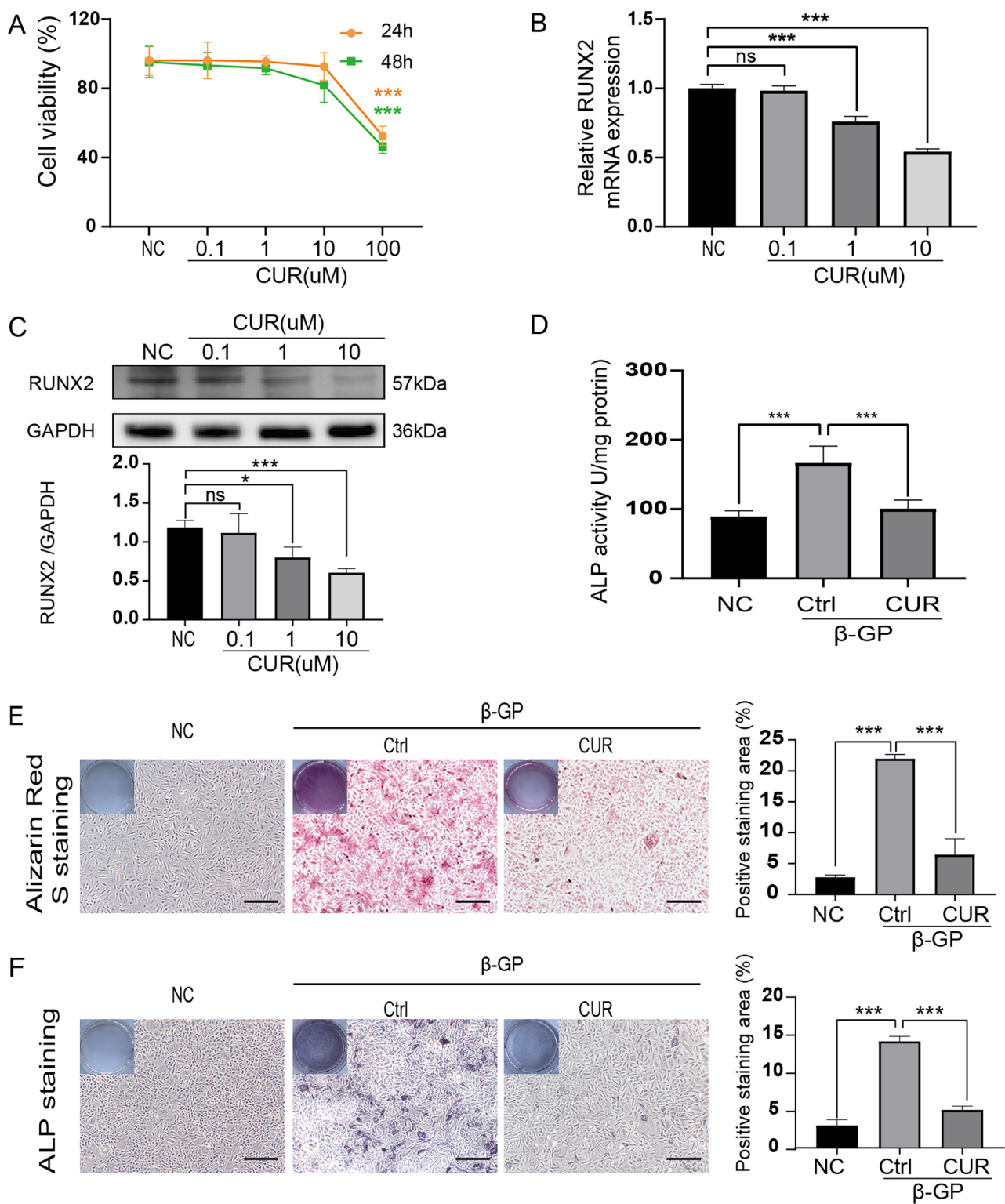
Figure 1. CUR attenuates the calcification of VSMCs. (A) Cell viability of VSMCs measured at 24 h and 48 h after incubation with different concentrations of CUR (0, 0.1, 1, 10, 100 μM). (B and C) Expression of RUNX2 measured after incubation of VSMCs with different concentrations of CUR (0, 0.1, 1, 10 μM). (B) RUNX2 mRNA expression. (C) RUNX2 protein expression. (D to F), VSMCs cultured in media supplemented with negative control, β-GP, or CUR + β-GP. (D) Alkaline phosphatase activity assay. (E) Six-well plates of cultured VSMCs subjected to Alizarin Red S staining, photographed as a whole with a cell phone and partially with a light microscope. The scale bar represents 200 μm. Positively stained regions were analyzed using Image J software. (F) Six-well plates of cultured VSMCs stained for alkaline phosphatase and photographed as a whole with a cell phone and partially with a light microscope. Positively stained regions were analyzed by Image J software. The scale bar stands for 200 μm. $*p < 0.05$, $**p < 0.01$, $***p < 0.001$. (A color version of this figure is available in the online journal.)

play a vital regulatory role in VC. Using RT-qPCR, we detected several miRNAs associated with calcification (miR-7a-5p, miR-92b-3p) and found that miR-92b-3p was expressed with a greater level in exosomes secreted after CUR intervention (Figure 4(A)). Similarly, miR-92b-3p was also highly expressed in CUR-intervened VSMCs (Figure 4(B)). To confirm that
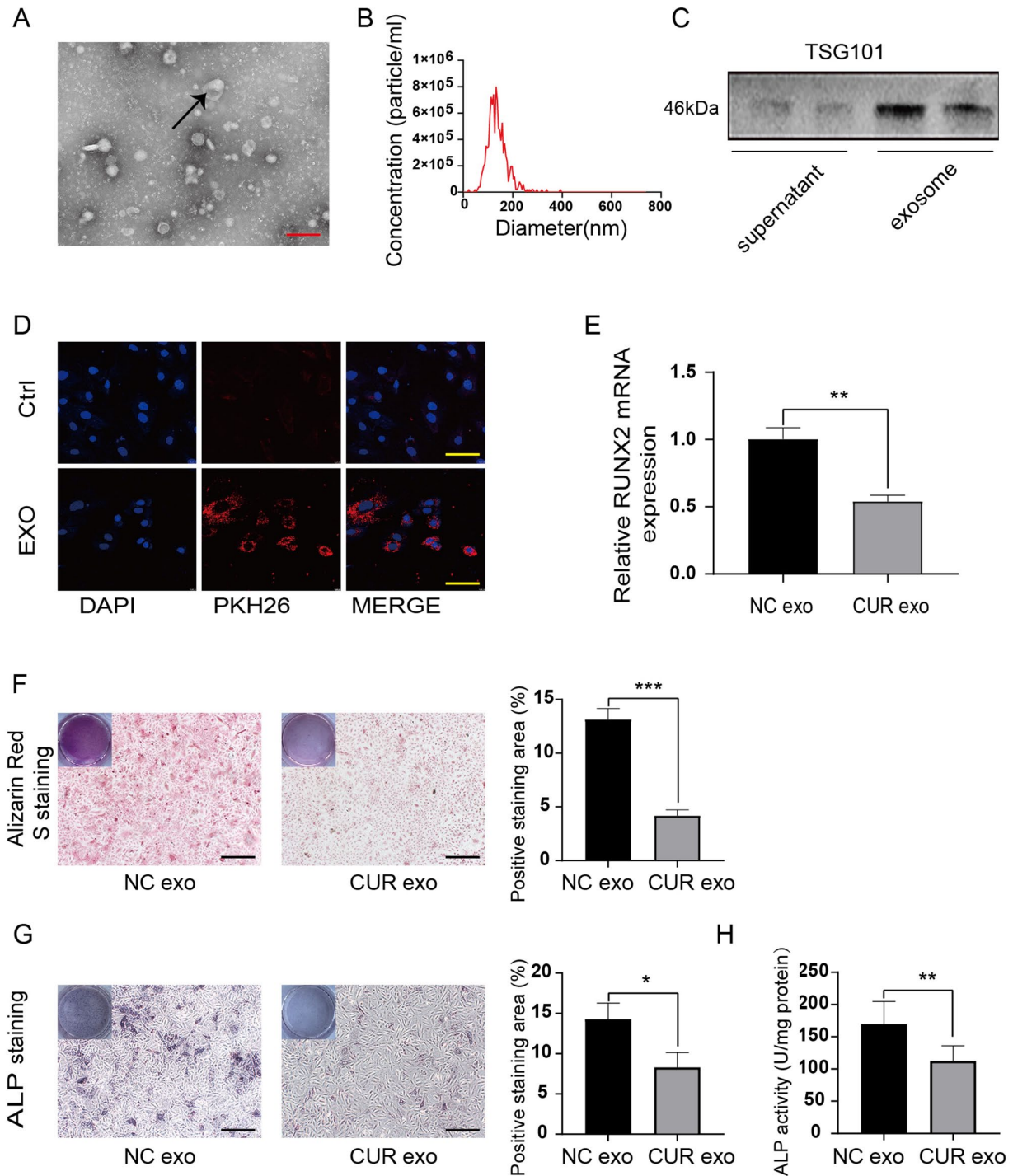
Figure 2. Exosomes secreted after CUR intervention in VSMCs inhibit the calcification of VSMCs. (A) Transmission electron microscopy images of exosomes. The scale bar represents 200 nm (red). (B) Nanoparticle tracking analysis of exosomes. (C) Western blot analysis showing that exosomes highly express TSG101 compared with that in the cell supernatant. (D) Confocal micrograph of PKH26-labeled exosomes or PBS (negative control) after co-culture with VSMCs for 12 h. The scale bar represents 40 μm (yellow). (E to H) Comparison of calcified VSMCs cultured with or without exosomes secreted by CUR-intervened calcified VSMCs. (E) Relative RUNX2 mRNA expression. (F) Alizarin Red S staining of cells. The positive staining areas were measured using Image J software. The scale bar represents 200 μm. (G) Cells were stained with alkaline phosphatase and the positive staining areas measured with ImageJ software. The scale bar represents 200 μm. (H) ALP activity assay. $*p < 0.05$, $**p < 0.01$, $***p < 0.001$. (A color version of this figure is available in the online journal.)

miR-92b-3p attenuated calcification in VSMCs, we transfected miR-92b-3p mimics into VSMCs. RT-qPCR showed that miR-92b-3p was significantly upregulated in VSMCs (Figure 4(C)). Fluorescence microscopy proved that the miR-92b-3p mimic was taken up by VSMCs (Figure 4(D)). To validate the regulatory role of miR-92b-3p in VC, we transfected the

cells with miR-92b-3p mimic and miR-92b-3p inhibitor and their corresponding controls. As shown in Figure 4(E) and (F), transfection of VSMCs with miR-92b-3p mimics decreased RUNX2 mRNA and protein expression, while transfection with the miR-92b-3p inhibitor increased expression. We suggest that VSMCs secrete exosomes containing high levels of
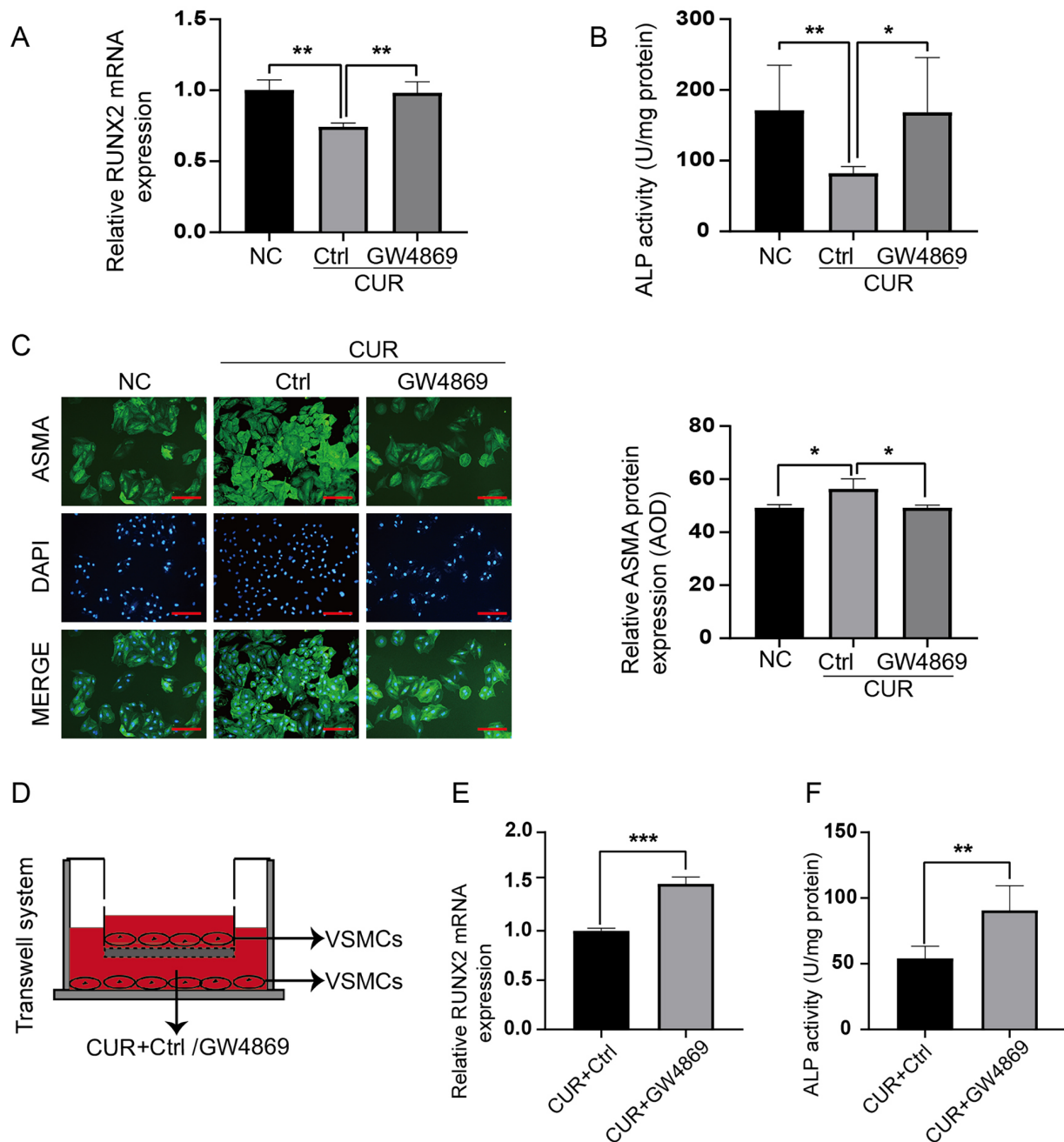
Figure 3. CUR affects exosomes secreted by VSMCs and attenuates the calcification of VSMCs. (A to C) VSMCs cultured with the media supplemented with negative control, CUR, or CUR + GW4869. (A) Relative RUNX2 mRNA expression. (B) ALP activity assay. (C) Immunofluorescence of ASMA and measurement of average optical density (AOD) using ImageJ software. The scale bar represents 100 μm. (D) Schematic diagram of the Transwell co-culture system used to analyze the interaction between exosomes in VSMCs. (E and F) VSMCs were cultured in the lower chamber of this system in medium supplemented with CUR, with or without GW4869, and co-cultured with normally growing VSMCs in the upper chamber. (E) Relative RUNX2 mRNA expression. (F) ALP activity assay. *$p < 0.05$, **$p < 0.01$, ***$p < 0.001$. (A color version of this figure is available in the online journal.)

miR-92b-3p after CUR intervention, which plays a role in attenuating calcification in VSMCs.

KLF4 is a target gene regulated by miR-92b-3p and is involved in the calcification of VSMCs

We used multiple bioinformatic databases to predict the downstream binding regulatory sites of miR-92b-3p. The combined results indicated that KLF4 was the highest scoring target (Figure 5(A)). To confirm whether miR-92b-3p can bind to KLF4 3′ UTR, we constructed the predicted miRNA binding sites containing wild-type or mutant KLF4 (WT-pMIR-KLF4 and MUT- pMIR-KLF4) in the luciferase reporter gene assay. As shown in Figure 5(B), transfection with the miR-92b-3p mimic did not affect the luciferase activity of VSMCs cells. The miR-92b-3p mimic inhibited KLF4 3′-UTR luciferase activity, while MUT- pMIR-KLF4 eliminated this inhibition. These data suggest that
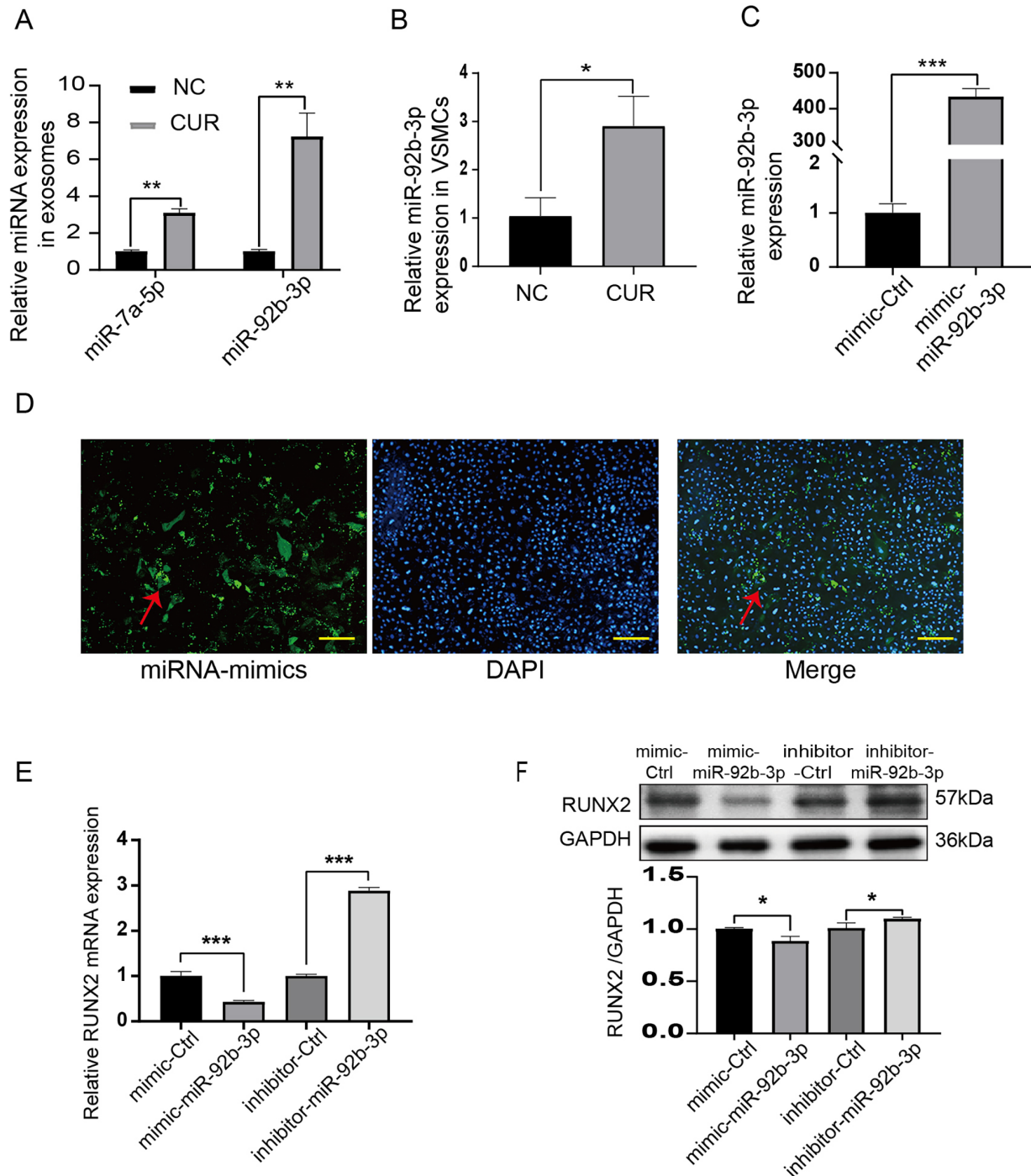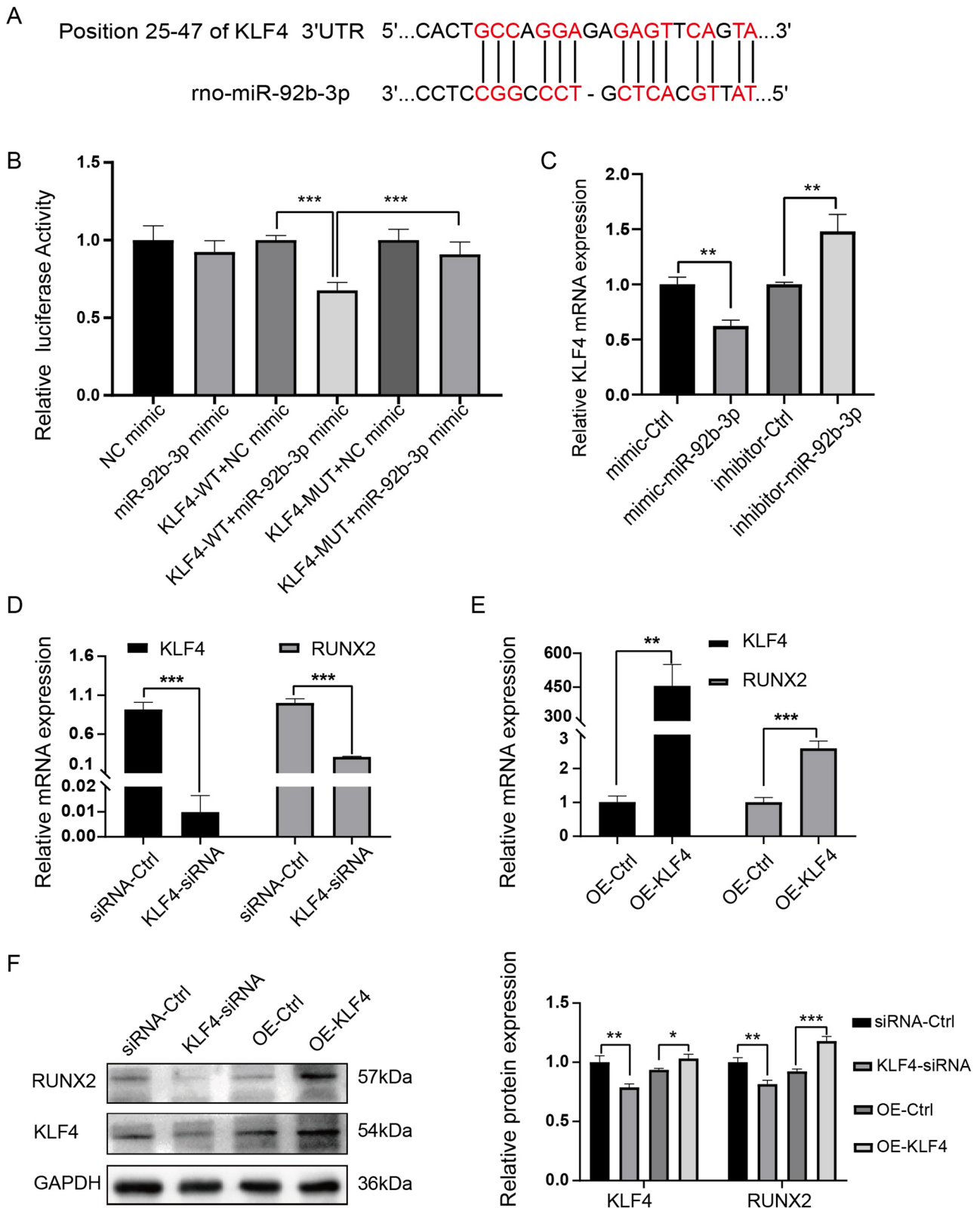
Figure 4. After VSMCs were incubated with CUR, the expression of miR-92b-3p was increased, which in turn suppressed the calcification of VSMCs. (A) Relative miRNA expression in exosomes after CUR intervention. (B) Relative miR-92b-3p expression in VSMCs after CUR intervention. (C) RT-qPCR results showing the efficiency of transfection with the miR-92b-3p mimic. (D) Fluorescence microscopy showing transfection with the miR-92b-3p mimic. The scale bar represents 200 μm (yellow). (E and F) Verification of the regulatory role of miR-92b-3p in VC, transfected with mimic control, miR-92b-3p mimic, inhibitor control, and miR-92b-3p inhibitors. (E) Relative RUNX2 mRNA expression. (F) Relative RUNX2 protein expression. *$p < 0.05$, **$p < 0.01$, ***$p < 0.001$. (A color version of this figure is available in the online journal.)

miR-92b-3p directly targets the 3′ UTR of KLF4. The results of RT-qPCR showed that the miR-92b-3p mimic reduced the expression of KLF4 mRNA, while the inhibitor increased this expression (Figure 5(C)).

We verified whether this was related to the calcification of VSMCs by inhibiting or overexpressing KLF4. The results of RT-qPCR confirmed that the expression of KLF4 mRNA in VSMCs decreased markedly after transfection with KLF4 siRNA, accompanied by a decline in the expression of osteogenic factor RUNX2 mRNA (Figure 5(D)). Meanwhile, we analyzed the RT-qPCR results to show that the expression of KLF4 mRNA increased dramatically after transfection with plasmids overexpressing KLF4, accompanied by an increase in the expression of osteogenic factor RUNX2 mRNA in VSMCs (Figure 5(E)). Western blot analysis validated the above results (Figure 5(F)).

A

Position 25-47 of KLF4 3'UTR 5'...CACTGCCAGGAGAGAGTTCAGTA...3'

rno-miR-92b-3p 3'...CCTCCGGCCCT - GCTCACGTTAT...5'

Figure 5. KLF4 is a target gene regulated by miR-92b-3p and is involved in the calcification of VSMCs. (A) Prediction of the binding site of miR-92b-3p to KLF4 3′ UTR using the RNA22 database. (B) Luciferase reporter analysis in HEK293T cells using WT or MUT carrying KLF4 3′ UTR to certify the regulatory relationship between miR-92b-3p and KLF4. (C) RT-qPCR showing that transfection with the miR-92b-3p mimic and miR-92b-3p inhibitor regulated the expression of KLF4 mRNA. Expression of RUNX2 mRNA in RT-qPCR results after transfection with KLF4 siRNA (D) or KLF4 plasmid (E) in VSMCs. (F) Relative protein expression of RUNX2 after KLF4 siRNA and overexpression of KLF4 plasmid intervention in VSMCs. $*p < 0.05$, $**p < 0.01$, $***p < 0.001$. (A color version of this figure is available in the online journal.)

CUR attenuates vascular calcification by increasing the expression of miR-92b-3p in the aorta

To demonstrate the effect of CUR on VC in rats, we prepared the following subgroups for comparison; negative control group, calcified control group, and CUR-treated calcified group. A schematic flow chart of the rat experiment is shown in Figure 6(A). Rat thoracic aorta was extracted for RT-qPCR analysis that showed the expression of miR-92b-3p was decreased in calcified aorta compared with that in the negative control (Figure 6(B)). The expression of both RUNX2 and KLF4 mRNA was significantly higher compared with that in the negative control (Figure 6(C)). Meanwhile, correlation analysis showed a negative correlation between the expression of KLF4 mRNA and miR-92b-3p ($r = -0.664$, $p = 0.0002$), as shown in Figure 6(D). The size of positive areas of Von Kossa staining and Alizarin Red S staining (Figure 6(E)), as with the expression levels of RUNX2 and KLF4 proteins in immunohistochemical assays (Figure 6(F)), was significantly higher in the calcification control group compared with that observed in the negative control group. These results indicate that the establishment of the rat vascular calcification model was successful. However, these effects were attenuated in the CUR-treated calcification group. In summary, CUR attenuated vitamin D3-induced VC by increasing miR-92b-3p expression and decreasing KLF4 expression in the aorta.

Discussion

This study showed that CUR attenuates vascular calcification via the exosomal miR-92b-3p/KLF4 axis. The study proposes a molecular mechanism for the attenuation of VC caused by exosome secretion. The expression of miRNAs to attenuate VC was mediated by the exchange of exosomes between VSMCs. We discovered that miR-92b-3p in exosomes and VSMCs were increased significantly when CUR affected VSMCs and targeted the expression of KLF4 to attenuate VC. Therefore, we conclude that CUR inhibits VC by increasing the content of miR-92b-3p in exosomes secreted by VSMCs, thereby regulating the expression of KLF4. The expression of KLF4 also influences the expression of osteogenic factor RUNX2 to regulate vascular calcification.

With the development of traditional Chinese medicine, the treatment of diseases by herbal medicine is receiving increased attention. It has been shown that CUR has protective effects on the cardiovascular system, with its effect on atherosclerosis through regulation of cholesterol metabolism, low-density lipoprotein (LDL) oxidation, and inflammatory factors having been widely reported.[27,28] Long-term CUR treatment lowers the level of blood lipids and liver cholesterol, thereby reducing the progression of atherosclerotic lesions.[29] The middle aortic layer is composed mainly of VSMCs with elastic fibers, with phenotypic transition, differentiation, and apoptosis of these cells related closely to VC. While there is evidence that CUR attenuates calcification in VSMCs by inhibiting the JNK/Bax signaling pathway,[14] its effect on VC remains unclear. In a study on the effects of CUR on glomerulonephritis by Gaedeke,[30] they used CUR at doses of 10, 50, 100, and 200 mg/kg and found

that a concentration of 50 mg resulted in the most significant reduction in the production of transforming growth factor beta (TGF-β),[30] which plays a very close role in VC.[31] In addition, in our preliminary experiments, we found that CUR at a concentration of 100 mg/kg was not readily absorbed by rats. Meanwhile, to avoid the toxicity of long-term CUR administration to rats, we chose a dose of 50 mg/kg for our *in vivo* experiments. Our study showed that supplementation with CUR *in vitro* and *in vivo* attenuated VC.

Exosomes are extracellular vesicles produced by many cells that contain miRNAs, mRNAs, and proteins having an essential role in intercellular communication by transporting various biological active substances to other cells, under both physiological and pathological conditions.[32] It has been shown that in a pathological setting VSMCs secrete calcified extracellular vesicles, which contain more calcification-related markers and fewer inhibitors of calcification, and that calcified extracellular vesicles induce increases in bone-derived genes (RUNX2, SMAD1, SP7)[33] which promote osteogenic differentiation and calcification in normal VSMCs.[21,34] Extracellular vesicles have also been reported to induce medial arterial calcification resulting in the accelerated VC observed in chronic kidney disease patients.[35] In this study, we extracted exosomes secreted after CUR intervention in VSMCs, and demonstrated, by using PKH26 labeling, that they could be absorbed by VSMCs. We also found that exosomes secreted after CUR intervention in VSMCs inhibited the calcification of VSMCs, although the addition of GW4869 weakened this impact. In addition, the Transwell co-culture system showed increased RUNX2 expression and ALP activity in VSMCs in the upper chamber in the CUR plus GW4869 treatment group compared with that observed in the CUR plus vector group. These findings prove that CUR inhibits the calcification of VSMCs by affecting the exosomes secreted from VSMCs.

Exosomes are rich in miRNAs that have a significant effect on intercellular communication. There is proof that miRNAs bind to the mRNA 3′UTR region and regulate mRNA expression for biological functions and that miR-29b-3p regulates VC via gelatinase matrix metalloproteinase-2.[36] In addition, miR-182 adjusts the calcification of VSMCs through regulation of SORT1.[24] Our experiments identified increased production of miR-92b-3p after CUR intervention in VSMCs. Some studies have demonstrated that miR-92b-3p is involved in the proliferation of VSMCs[37,38] and is also involved in ovarian cancer tumor growth and tumor-associated angiogenesis.[39] Validation by bioinformatic prediction and the dual luciferase gene reporter assay led us to conclude that the target for the miR-92b-3p-regulation might be KLF4. KLF4 is an important transcription factor, located mainly in the nucleus, with the ability to regulate VSMC phenotype.[40] KLF4 has been reported to activate the transcription factor RUNX2 to induce VC.[41–43] In addition, KLF4 regulates vascular calcification via the Jak/Stat signaling pathway.[44] Our experiments showed that the activity of the osteogenic factor RUNX2 was decreased or increased by inhibition or overexpression of KLF4, respectively. On the basis of these results, we suggest that CUR affects exosomes secreted from VSMCs that are rich in miR-92b-3p, which in turn, play a vital role in VC by adjusting the expression of KLF4.
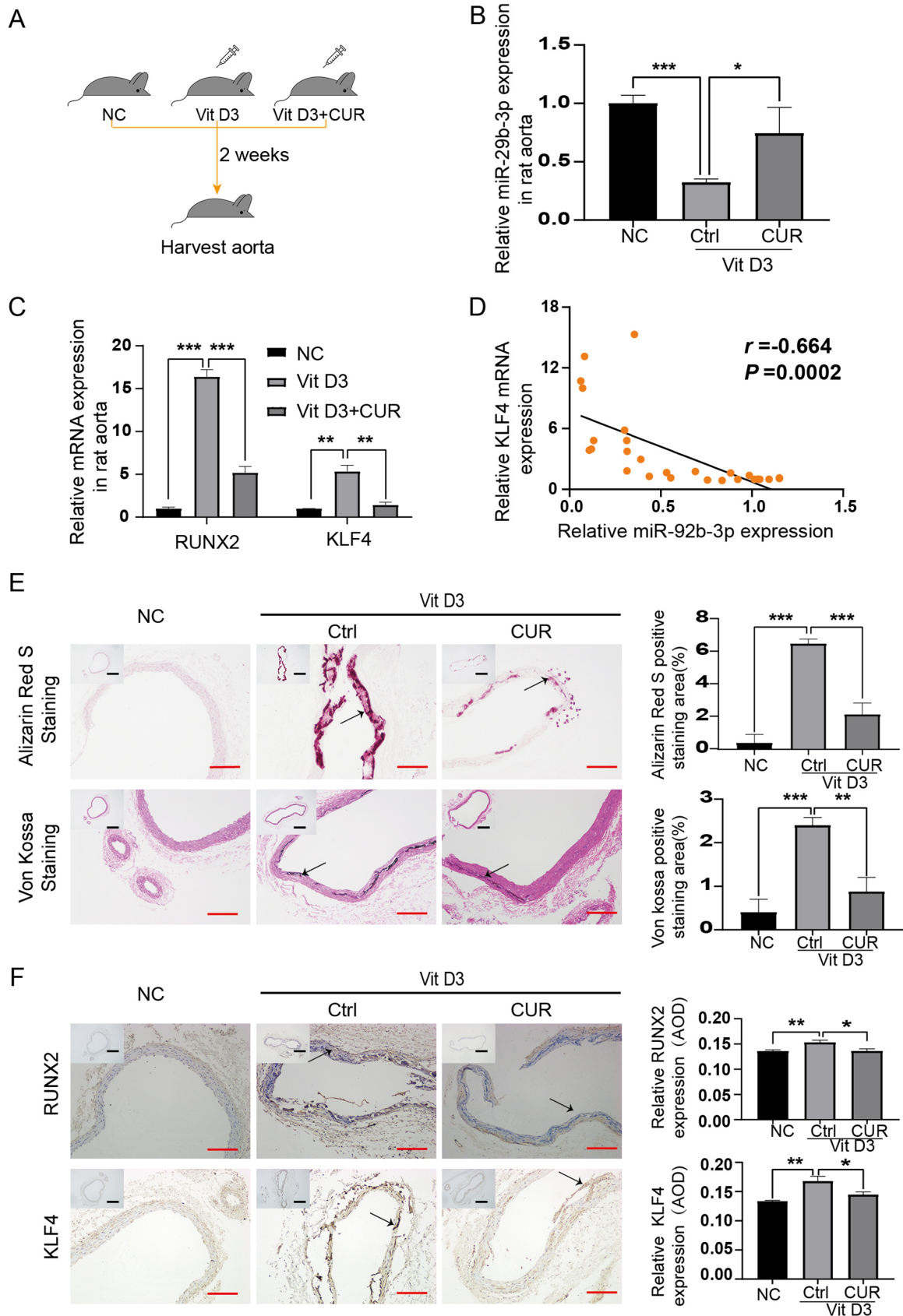
Figure 6. CUR attenuates vascular calcification by increasing the expression of miR-92b-3p in the aorta. (A) Schematic diagram of the intervention model for rats in animal experiments. Relative expressions in RT-qPCR of miR-92b-3p (B) and RUNX2 and KLF4 mRNA (C) in rat aorta. (D) Correlation analysis of KLF4 mRNA and miR-92b-3p expression. (E) Alizarin Red S-staining and Von Kossa staining of rat aorta. The positively stained regions were analyzed using ImageJ software. The scale bar represents 500 μm (black) and 200 μm (red). (F) Expression of RUNX2 and KLF4 proteins in the thoracic artery detected by immunohistochemistry and the mean optical density values analyzed by ImageJ software. The scale bar represents 500 μm (black) and 200 μm (red). $*p < 0.05$, $**p < 0.01$, $***p < 0.001$. (A color version of this figure is available in the online journal.)

Conclusions

Our study showed that CUR attenuates VC via the exosomal miR-92b-3p/KLF4 axis. CUR attenuates VC by affecting the exosomes secreted by VSMCs, which provides us with a new option for the treatment and prevention of this vascular abnormality. However, our experiments had some limitations in that we did not carry out *in vivo* experiments on the possible inhibitory effects of miR-92b-3p on VC. The pathogenesis of VC is complex. Whether vitamin D3 and β-glycerophosphate that have been used as models of calcification *in vivo* and *in vitro* are applicable to VC caused by various diseases needs to be investigated further. In future studies, we plan to use agomir miR-92b-3p and antagomir miR-92b-3p to validate the effect of miR-92b-3p on VC caused by vitamin D3 and chronic kidney disease, respectively.

AUTHORS' CONTRIBUTIONS

All the authors participated in the design, interpretation of the studies and analysis of the data, and review of the manuscript. CZC, YDL, and XQ designed the study. CZC, YDL, and HLL performed the experiments, analyzed the data, and wrote the paper. KL, ZMZ, WHJ, and XQ instructed the experimental methods and revised the manuscript. All authors provided feedback and approved the final version of the manuscript.

DECLARATION OF CONFLICTING INTERESTS

The author(s) declared no potential conflicts of interest with respect to the research, authorship, and/or publication of this article.

FUNDING

ORCID IDS

Chuanzhen Chen (iD) https://orcid.org/0000-0001-6970-9446
Xiao Qin (iD) https://orcid.org/0000-0002-2161-0735

REFERENCES

1. Durham AL, Speer MY, Scatena M, Giachelli CM, Shanahan CM. Role of smooth muscle cells in vascular calcification: implications in atherosclerosis and arterial stiffness. *Cardiovasc Res* 2018;**114**:590–600

2. Chow B, Rabkin SW. The relationship between arterial stiffness and heart failure with preserved ejection fraction: a systemic meta-analysis. *Heart Fail Rev* 2015;**20**:291–303

3. Steitz SA, Speer MY, Curinga G, Yang HY, Haynes P, Aebersold R, Schinke T, Karsenty G, Giachelli CM. Smooth muscle cell phenotypic transition associated with calcification: upregulation of Cbfa1 and downregulation of smooth muscle lineage markers. *Circ Res* 2001;**89**:1147–54

4. Rodríguez A, Frühbeck G, Gómez-Ambrosi J, Catalán V, Sáinz N, Díez J, Zalba G, Fortuño A. The inhibitory effect of leptin on angiotensin II-induced vasoconstriction is blunted in spontaneously hypertensive rats. *J Hypertens* 2006;**24**:1589–97

5. Iyemere VP, Proudfoot D, Weissberg PL, Shanahan CM. Vascular smooth muscle cell phenotypic plasticity and the regulation of vascular calcification. *J Intern Med* 2006;**260**:192–210

6. Jiang W, Zhang Z, Li Y, Chen C, Yang H, Lin Q, Hu M, Qin X. The cell origin and role of osteoclastogenesis and osteoblastogenesis in vascular calcification. *Front Cardiovasc Med* 2021;**8**:639740

7. Yang X, Thomas DP, Zhang X, Culver BW, Alexander BM, Murdoch WJ, Rao MN, Tulis DA, Ren J, Sreejayan N. Curcumin inhibits platelet-derived growth factor-stimulated vascular smooth muscle cell function and injury-induced neointima formation. *Arterioscler Thromb Vasc Biol* 2006;**26**:85–90

8. Hasan ST, Zingg JM, Kwan P, Noble T, Smith D, Meydani M. Curcumin modulation of high fat diet-induced atherosclerosis and steatohepatosis in Ldl receptor deficient mice. *Atherosclerosis* 2014;**232**:40–51

9. Zhang D, Yang Y, Li Y, Zhang G, Cheng Z. Inhibitory effect of curcumin on artery restenosis following carotid endarterectomy and its associated mechanism in vitro and in vivo. *Drug Des Devel Ther* 2020;**14**:855–66

10. Meng Z, Yan C, Deng Q, Gao DF, Niu XL. Curcumin inhibits LPS-induced inflammation in rat vascular smooth muscle cells in vitro via Ros-relative Tlr4-Mapk/NF-κB pathways. *Acta Pharmacol Sin* 2013;**34**:901–11

11. Hao F, Kang J, Cao Y, Fan S, Yang H, An Y, Pan Y, Tie L, Li X. Curcumin attenuates palmitate-induced apoptosis in Min6 pancreatic β-cells through PI3K/Akt/FoxO1 and mitochondrial survival pathways. *Apoptosis* 2015;**20**:1420–32

12. Proudfoot D, Skepper JN, Hegyi L, Bennett MR, Shanahan CM, Weissberg PL. Apoptosis regulates human vascular calcification in vitro: evidence for initiation of vascular calcification by apoptotic bodies. *Circ Res* 2000;**87**:1055–62

13. Shroff RC, Mcnair R, Figg N, Skepper JN, Schurgers L, Gupta A, Hiorns M, Donald AE, Deanfield J, Rees L, Shanahan CM. Dialysis accelerates medial vascular calcification in part by triggering smooth muscle cell apoptosis. *Circulation* 2008;**118**:1748–57

14. Hou M, Song Y, Li Z, Luo C, Ou JS, Yu H, Yan J, Lu L. Curcumin attenuates osteogenic differentiation and calcification of rat vascular smooth muscle cells. *Mol Cell Biochem* 2016;**420**:151–60

15. Fleenor BS, Sindler AL, Marvi NK, Howell KL, Zigler ML, Yoshizawa M, Seals DR. Curcumin ameliorates arterial dysfunction and oxidative stress with aging. *Exp Gerontol* 2013;**48**:269–76

16. Zhao JF, Ching LC, Huang YC, Chen CY, Chiang AN, Kou YR, Shyue SK, Lee TS. Molecular mechanism of curcumin on the suppression of cholesterol accumulation in macrophage foam cells and atherosclerosis. *Mol Nutr Food Res* 2012;**56**:691–701

17. Hutcheson JD, Goettsch C, Bertazzo S, Maldonado N, Ruiz JL, Goh W, Yabusaki K, Faits T, Bouten C, Franck G, Quillard T, Libby P, Aikawa M, Weinbaum S, Aikawa E. Genesis and growth of extracellular-vesicle-derived microcalcification in atherosclerotic plaques. *Nat Mater* 2016;**15**:335–43

18. Pegtel DM, Gould SJ. Exosomes. *Annual Review of Biochemistry* 2019;**88**:487–514

19. Kapustin AN, Chatrou ML, Drozdov I, Zheng Y, Davidson SM, Soong D, Furmanik M, Sanchis P, de Rosales RT, Alvarez-Hernandez D, Shroff R, Yin X, Muller K, Skepper JN, Mayr M, Reutelingsperger CP, Chester A, Bertazzo S, Schurgers LJ, Shanahan CM. Vascular smooth muscle cell calcification is mediated by regulated exosome secretion. *Circ Res* 2015;**116**:1312–23

20. Shanahan CM, Cary NR, Salisbury JR, Proudfoot D, Weissberg PL, Edmonds ME. Medial localization of mineralization-regulating proteins in association with Mönckeberg's sclerosis: evidence for smooth muscle cell-mediated vascular calcification. Circulation 1999;**100**:2168–76

21. Krohn JB, Hutcheson JD, Martínez-Martínez E, Aikawa E. Extracellular vesicles in cardiovascular calcification: expanding current paradigms. *J Physiol* 2016;**594**:2895–903

22. Chen NX, O'Neill KD, Moe SM. Matrix vesicles induce calcification of recipient vascular smooth muscle cells through multiple signaling pathways. *Kidney Int* 2018;**93**:343–54

23. Yuan C, Ni L, Zhang C, Hu X, Wu X. Vascular calcification: new insights into endothelial cells. *Microvasc Res* 2021;**134**:104105

24. Zhang Z, Jiang W, Yang H, Lin Q, Qin X. The miR-182/Sort1 axis regulates vascular smooth muscle cell calcification in vitro and in vivo. *Exp Cell Res* 2018;**362**:324–31

25. Chang JR, Guo J, Wang Y, Hou YL, Lu WW, Zhang JS, Yu YR, Xu MJ, Liu XY, Wang XJ, Guan YF, Zhu Y, Du J, Tang CS, Qi YF.

Intermedin1-53 attenuates vascular calcification in rats with chronic kidney disease by upregulation of α-Klotho. *Kidney Int* 2016;**89**:586–600

26. Xu F, Zhong JY, Lin X, Shan SK, Guo B, Zheng MH, Wang Y, Li F, Cui RR, Wu F, Zhou E, Liao XB, Liu YS, Yuan LQ. Melatonin alleviates vascular calcification and ageing through exosomal miR-204/miR-211 cluster in a paracrine manner. *J Pineal Res* 2020;**68**:e12631

27. Panahi Y, Ahmadi Y, Teymouri M, Johnston TP, Sahebkar A. Curcumin as a potential candidate for treating hyperlipidemia: a review of cellular and metabolic mechanisms. *J Cell Physiol* 2018;**233**:141–52

28. Sundar Dhilip Kumar S, Houreld NN, Abrahamse H. Therapeutic potential and recent advances of curcumin in the treatment of aging-associated diseases. *Molecules (Basel, Switzerland)* 2018;**23**:835

29. Shin SK, Ha TY, McGregor RA, Choi MS. Long-term curcumin administration protects against atherosclerosis via hepatic regulation of lipoprotein cholesterol metabolism. *Mol Nutr Food Res* 2011;**55**:1829–40

30. Gaedeke J, Noble NA, Border WA. Curcumin blocks fibrosis in anti-Thy 1 glomerulonephritis through up-regulation of heme oxygenase 1. *Kidney Int* 2005;**68**:2042–9

31. Yang P, Troncone L, Augur ZM, Kim SSJ, McNeil ME, Yu PB. The role of bone morphogenetic protein signaling in vascular calcification. *Bone* 2020;**141**:115542

32. Lin X, Li S, Wang YJ, Wang Y, Zhong JY, He JY, Cui XJ, Zhan JK, Liu YS. Exosomal Notch3 from high glucose-stimulated endothelial cells regulates vascular smooth muscle cells calcification/aging. *Life Sci* 2019;**232**:116582

33. Nishimura R, Wakabayashi M, Hata K, Matsubara T, Honma S, Wakisaka S, Kiyonari H, Shioi G, Yamaguchi A, Tsumaki N, Akiyama H, Yoneda T. Osterix regulates calcification and degradation of chondrogenic matrices through matrix metalloproteinase 13 (MMP13) expression in association with transcription factor Runx2 during endochondral ossification. *The Journal of Biological Chemistry* 2012;**287**:33179–90

34. Yang W, Zou B, Hou Y, Yan W, Chen T, Qu S. Extracellular vesicles in vascular calcification. *Clin Chim Acta; Int J Clin Chem* 2019;**499**:118–22

35. Viegas CSB, Santos L, Macedo AL, Matos AA, Silva AP, Neves PL, Staes A, Gevaert K, Morais R, Vermeer C, Schurgers L, Simes DC. Chronic kidney disease circulating calciprotein particles and extracellular vesicles promote vascular calcification: a role for Grp (Gla-Rich Protein). *Arterioscler Thromb Vasc Biol* 2018;**38**:575–87

36. Jiang W, Zhang Z, Yang H, Lin Q, Han C, Qin X. The involvement of miR-29b-3p in arterial calcification by targeting matrix metalloproteinase-2. *Biomed Res Int* 2017;**2017**:6713606

37. Wu ZB, Cai L, Lin SJ, Lu JL, Yao Y, Zhou LF. The miR-92b functions as a potential oncogene by targeting on Smad3 in glioblastomas. *Brain Res* 2013;**1529**:16–25

38. Lee J, Heo J, Kang H. miR-92b-3p-TSC1 axis is critical for mTOR signaling-mediated vascular smooth muscle cell proliferation induced by hypoxia. *Cell Death Differ* 2019;**26**:1782–95

39. Wang J, Wang C, Li Y, Li M, Zhu T, Shen Z, Wang H, Lv W, Wang X, Cheng X, Xie X. Potential of peptide-engineered exosomes with overexpressed miR-92b-3p in anti-angiogenic therapy of ovarian cancer. *Clin Transl Med* 2021;**11**:e425

40. Davis-Dusenbery BN, Chan MC, Reno KE, Weisman AS, Layne MD, Lagna G, Hata A. Down-regulation of Kruppel-like factor-4 (KLF4) by microRNA-143/145 is critical for modulation of vascular smooth muscle cell phenotype by transforming growth factor-beta and bone morphogenetic protein 4. *J Biol Chem* 2011;**286**:28097–110

41. Zhu L, Zhang N, Yan R, Yang W, Cong G, Yan N, Ma W, Hou J, Yang L, Jia S. Hyperhomocysteinemia induces vascular calcification by activating the transcription factor Runx2 via Krüppel-like factor 4 up-regulation in mice. *J Biol Chem* 2019;**294**:19465–74

42. Song Y, Hou M, Li Z, Luo C, Ou JS, Yu H, Yan J, Lu L. Tlr4/NF-κB/Ceramide signaling contributes to Ox-LDL-induced calcification of human vascular smooth muscle cells. *Eur J Pharmacol* 2017;**794**:45–51

43. Yoshida T, Yamashita M, Hayashi M. Kruppel-like factor 4 contributes to high phosphate-induced phenotypic switching of vascular smooth muscle cells into osteogenic cells. *J Biol Chem* 2012;**287**:25706–14

44. Lin L, He Y, Xi BL, Zheng HC, Chen Q, Li J, Hu Y, Ye MH, Chen P, Qu Y. MiR-135a suppresses calcification in senescent VSMCs by regulating Klf4/Stat3 pathway. *Curr Vasc Pharmacol* 2016;**14**:211–8